J Mater Sci (2010) 45:6025–6029
DOI 10.1007/s10853-010-4686-y

The presence of fivefold germanium as a possible transitional phase in the iron–lead–germanate glass system

S. Rada · R. Chelcea · E. Culea

Received: 11 February 2010 / Accepted: 31 May 2010 / Published online: 16 June 2010

Abstract Glasses in the system $x\text{Fe}_2\text{O}_3\cdot(100-x)[7\text{GeO}_2\cdot3\text{PbO}]$ with $0 \leq x \leq 60$ mol% have been prepared from melt quenching method. In this article, we investigated changes in germanium coordination number in iron–lead–germanate glasses through molar volume analysis, measurements of densities, investigations of FTIR, and UV–VIS spectroscopy. The observations present in these mechanisms show that the lead ions have an affinity pronounced toward [GeO_5] and [FeO_4] structural units with non-bridging oxygens. The excess of oxygen can be supported into the glass network by the formation of [FeO_6] structural units and the apparition of the germanate anomaly. At higher content of iron (III) oxide, the anomaly behavior of the germanium is due to the formations of [FeO_6] structural units. Our results show that the presence of fivefold germanium as a possible transitional phase from four to sixfold germanium it is necessary for the formation of the [FeO_6] structural units and the apparition of the Fe_2O_3 crystalline phase. Pb^{+2} ions with $6s^2$ configuration show strong absorption in the ultraviolet due to parity allowed s^2-sp transition.

Introduction

Lead–germanate glasses are particularly interesting as they can be readily made in fiberglass form for use in the field of optical devices [1, 2]. The lead oxide is known as a non-conventional network former [3–5] which may play a dual role, both as a network modifier and a network former in the vitreous matrix [6, 7]. This role depends on the type of ionic or covalent bond between lead and oxygen atoms.

On the other hand, the germanate anomaly was observed in alkali–germanate glasses [8, 9]. The structural mechanism responsible for the anomaly remains an area of interest to the glass science. The currently accepted model for this mechanism is a change of germanium from 4-coordinated to higher coordinated species. The germanate anomaly consists in a growth followed by a decline of the number of [GeO_6] octahedral structural units in the glass network [9–13]. While the formation of the higher coordinated species clearly plays a role in the anomalous behavior it does not correlate with the anomaly maximum.

This effect is related to an untypical change of the glass properties such as glass transition temperature, viscosity, thermal expansion coefficient, electrical conductivity, density in the function of glass stoichiometry, and is quite common and well known in alkali–germanate glasses [13–15]. At the atomic level, the germanate anomaly is related to a change in the germanium ions neighborhood from a tetrahedral to an octahedral geometry. A different model suggested that the anomaly is associated with the longer Ge–O distances of [GeO_4] tetrahedrons and the effect these longer distances yield on the accommodation of the alkali metal cations in the network. In this model, the addition of small amounts of alkali-oxide causes formation of 3-membered rings of [GeO_4] tetrahedrons in the general vicinity of the alkali metal cations. These small rings create smaller network cavities [13–15].

The appearance of the germanate anomaly in germanate glasses doped with heavy-metal oxides as PbO remains an open question. Lead–germanate glasses show interesting optical properties [16–18] and it is expected that the introduction of an iron oxide component into the binary lead–germanate glasses may affect the structural features

S. Rada (✉) · R. Chelcea · E. Culea
Department of Physics, Technical University of Cluj-Napoca,
400020 Cluj-Napoca, Romania
e-mail: Simona.Rada@phys.utcluj.ro; radasimona@yahoo.com

of the host matrix. In this article, iron–lead–germanate glasses were studied to understand the structural mechanism responsible for the germanate anomaly.

Experimental

Glasses were prepared by mixing and melting appropriate amounts of lead (IV) oxide, germanium oxide (IV), and iron (III) oxide of high purity (99,99%, Aldrich Chemical Co.). Reagents were melted at 1000 °C at 15 min and quenched.

The samples were analyzed by means of X-ray diffraction using a XRD-6000 Shimadzu Diffractometer, with a monochromator of graphite for Cu K_α radiation ($\lambda = 1.54$ Å) at room temperature.

The FT-IR absorption spectra of the glasses in the 370–1250 cm^{-1} spectral range were obtained with a JASCO FTIR 6200 spectrometer using the standard KBr pellet disc technique. The spectra were carried out with a standard resolution of 2 cm^{-1}.

UV–Visible absorption spectra of the powdered glass samples were recorded at room temperature in the range 250–800 cm^{-1} using a Perkin-Elmer Lambda 45 UV/VIS spectrometer. These measurements were made on glass powder dispersed in KBr pellets.

Results and discussion

The X-ray diffraction patterns did not reveal any crystallinity in the samples with $x < 60$ mol% Fe_2O_3. However, at the composition $x = 60$ mol% Fe_2O_3 Bragg peaks associated with the Fe_2O_3 crystalline phase were observed, Fig. 1.

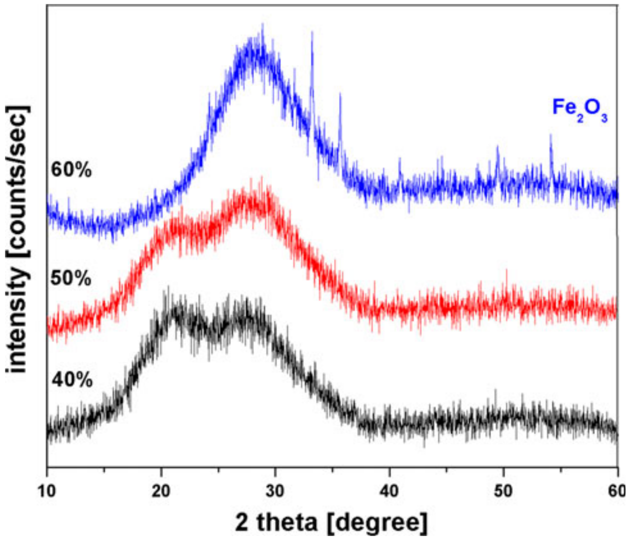

Fig. 1 X-ray diffraction patterns for $x\text{Fe}_2\text{O}_3\cdot(100 - x)[7\text{GeO}_2\cdot 3\text{PbO}_2]$ glass system with $x \geq 40$ mol%

FTIR spectroscopy

The examination of FTIR spectra of the $x\text{Fe}_2\text{O}_3\cdot(100 - x)[7\text{GeO}_2\cdot 3\text{PbO}_2]$ glasses exposed in Fig. 2 shows that the Fe_2O_3 content modifies the characteristic IR bands as follows:

(i) The bands situated at about 670 and 870 cm^{-1} can be attributed to the Pb–O bonds vibrations from $[PbO_3]$ and $[PbO_4]$ structural units [19–25]. According to the electronegativity theory, the covalency of the bond will become stronger with the decrease of the difference of electronegativity between cation and anion ions. Since the values of electronegativity, for Ge, Fe, Pb, and O elements are 1.96, 1.83, 2.33, and 3.5, respectively, the covalency of Pb–O is stronger than Ge–O and Fe–O, respectively. As a result, the higher affinity of the lead and germanium ions to attract oxygens atoms results in the formation of higher coordination Pb and Ge structural units. Then, the increase of the content of Fe^{+3} ions in the glass matrix needs the compensation of the charge with the oxygens ions by ionic bonds and produces the apparition of the Fe_2O_3 crystalline phase, in agreement with XRD data.

On the other hand, the presence of the Pb^{+2} ions charge compensation with structural units containing non-bridging oxygen occurs (such as $[GeO_5]$ or $[FeO_4]$ structural units). It seems likely that the band located at 700 cm^{-1}, arising from the presence of $[GeO_6]$ structural units, is reduced because the modified $[GeO_5]$ structural units containing one or more Ge–O–Pb bonds are unable to accept a sixth oxygen atom. The accumulation of oxygen atoms in the glass network can be supported by the conversion of $[GeO_4]$ to $[GeO_5]$ structural units.

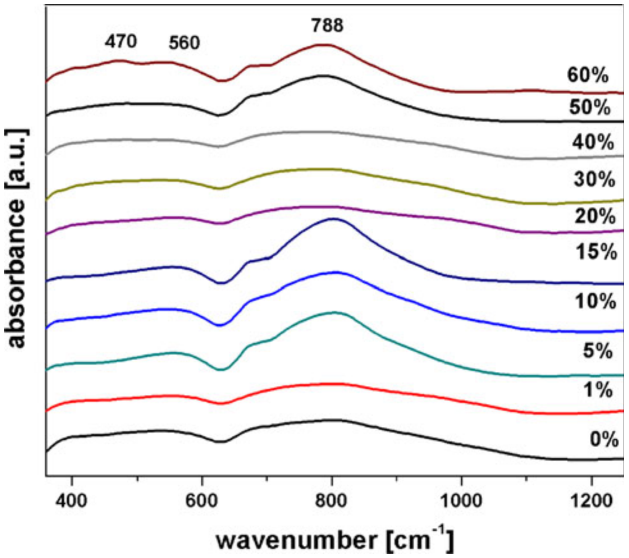

Fig. 2 FTIR spectra of $x\text{Fe}_2\text{O}_3\cdot(100 - x)[7\text{GeO}_2\cdot 3\text{PbO}_2]$ glasses with $0 \leq x \leq 60$ mol%

With increasing Fe_2O_3 content up to 15 mol%, the formation of larger numbers of non-bridging oxygen's results in the formation of $[PbO_n]$ structural units ($n = 3, 4$) in the vicinity of the $[GeO_5]$ structural units.

(ii) By increasing Fe_2O_3 content to 20 mol%, the intensity of the absorption bands typical of the $[GeO_4]$ structural units (~810 cm^{-1}) decreases [11–13, 25]. Thus, new band appears at about 560 cm^{-1} corresponding to the vibrations of the Fe–O bond in the $[FeO_4]$ structural units [23]. The prominent band located in the region between 850 and 1100 cm^{-1} consists of various overlapping bands which arise from the stretching and bending modes of the $[GeO_4]$, $[PbO_3]$, and $[PbO_4]$ structural units. Therefore, the decreasing intensity of the bands located in the 400–875 cm^{-1} region is a result of increasing polymerization of the iron–lead–germanate glass network.

A decreasing trend of the IR band located at about 700 cm^{-1} shows the conversion of some $[GeO_6]$ to $[GeO_5]$ structural units. On the other hand, the relative increase in the intensity of the IR band centered at about 560 cm^{-1} corresponding to the Fe–O bond in the $[FeO_4]^{-1}$ anions do not preserve the matrix connectivity and necessitates the rapid compensation with Pb^{+2} yielding drastic modifications in the IR spectra.

(iii) For sample with $20 \leq x \leq 40$ mol% Fe_2O_3, the degree of polymerization increases. The evolution of the structure can be explained by the conversion of some $[GeO_4]$ to $[GeO_6]$ structural units, which is driven by the need to accommodate additional oxygen in the glass system. We assume that $[GeO_n]$ structural units, where $n = 5, 6$ do not form bonds with non-bridging oxygens, thus yielding the formation of $[GeO_4]$ structural units [11–13]. The $[GeO_5]$ polyhedrons are suitable neighbors for the lead Pb^{+2} ions.

(iv) The increase of Fe_2O_3 content up to 60 mol% results in the conversion of some $[FeO_4]$ to $[FeO_6]$ structural units [26]. This is indicated by a new band situated at about 470 cm^{-1}, which is associated with vibrations of the Fe–O bond from $[FeO_6]$ structural units. A noticeable change appears also in the characteristic features of the $[GeO_4]$ structural units (band located at about 788 cm^{-1}). These modifications explain the conversion of some $[GeO_6]$ to $[GeO_4]$ structural units, while the $[FeO_4]$ structural units are transformed to the $[FeO_6]$ structural units. Then, a decreasing trend toward lower wavenumber was observed for the bands situated in the 650–980 cm^{-1} region. This may be attributed to the electrostatic field of the strongly polarizing Pb^{+2} ions. The increase of the Pb^{+2} ions content leads to the strengthening of the electron cloud around oxygens in the $[GeO_5]$ units and, consequently, causes a shift of stretching vibration of the Ge–O-Ge to lower wavenumbers.

Iron in the oxidation state +3 is reported to occur predominantly in fourfold coordination, as $[FeO_4]^{-1}$. These tetrahedral geometries have a negative charge and hence need cations, in the case of the glasses studied, Pb^{+2} for charge compensation. Accordingly, it is possible a better stabilization of Fe^{+3} from $[FeO_4]^{-1}$ tetrahedral geometry can be achieved through compensation with Pb^{+2} ions. The transformation of some $[FeO_4]$ to $[FeO_6]$ structural units results in some disposable lead ions which will increase the electrostatic field of the Pb^{+2} ions.

On the other hand, a growth followed by a decline of the number of $[GeO_6]$ octahedral structural units in the glass network constitutes the germanate anomaly. The currently accepted model for this mechanism is a change of the coordination of the germanium from 4-coordinated to higher coordinated species such as $[GeO_n]$ structural units where $n = 5$ and 6.

In brief, the lead ions are a unique influence on the structure of the iron–lead–germanate glasses. The lead atoms which form covalent bonds participate as network former, while the lead ions which form ionic bonds have a strong affinity toward $[GeO_5]$ and $[FeO_4]$ structural units containing non-bridging oxygens. The pronounced affinity toward germanate units yields the germanate anomaly. Then, the excess of oxygen can be supported into the glass network by the formation of $[FeO_6]$ structural units. The existence of the Pb^{+2} ions in the glasses network can be checked by means of UV–VIS spectroscopy. Lead ions with s^2 configuration absorb strongly in the ultraviolet and yield broad emission bands in the ultraviolet and blue spectral area.

UV–VIS spectroscopy

The UV–VIS absorption spectra of $xFe_2O_3 \cdot (100 - x)[7GeO_2 \cdot 3PbO_2]$ glasses with $x = 0$–60 mol% are shown in Fig. 3. An examination of these spectra shows that the characteristic UV–VIS bands are modified by the addition of Fe_2O_3 as follows:

(i) For all glasses, the UV absorption bands begin at 250 nm by an ascending lobe. These UV absorption bands are assumed to originate from lead germanate host matrix. The stronger transitions in the UV–VIS spectrum can be due to the presence of the Ge=O bonds from $[GeO_5]$ structural units and Pb=O bonds from $[PbO_3]$ structural units which allow n–π^* transitions. Pb^{+2} ions with s^2 configuration absorb strongly in the ultraviolet and yield broad emission bands in the ultraviolet and blue spectral area and the intense band obtained centered at about 310 nm corresponds to the Pb^{+2} ions [27].

(ii) The introduction of low concentrations of Fe_2O_3 ($x \leq 5$ mol%) into the host matrix results in the formation of new absorption UV bands between 320 and 450 nm. These bands arise from to the d–d transitions of the Fe^{+3} ions [28–35].

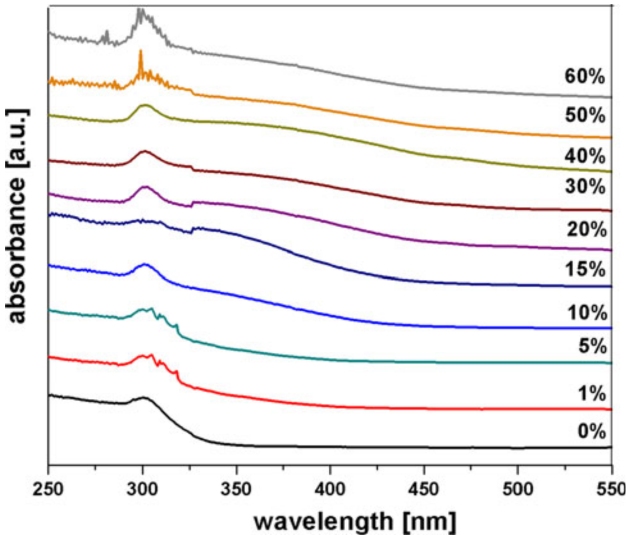

Fig. 3 UV–VIS absorption spectra of $x\mathrm{Fe_2O_3}\cdot(100-x)[7\mathrm{GeO_2}\cdot 3\mathrm{PbO_2}]$ glasses in function of iron oxide content

(iii) The addition of Fe_2O_3 content until 10 mol% causes a decrease in the intensity of the UV absorption bands situated in the 320–450 nm domain. This noticeable decrease can attributed to the iron ions acting as network former.

(iv) A further increase in the Fe_2O_3 content up to 20 mol% results in an increase in the intensity of the 250 nm band. This increase is due to the formation of new n–π^* transitions of the [O=GeO_4] structural units.

(v) For samples containing between $20 \leq x \leq 40$ mol% Fe_2O_3, the majority of Fe^{+3} d–d bands are observed in the 325–450 nm region [28–35]. The evolution of the structure can be explained by the conversion of some [FeO_4] to [FeO_6] structural units to accommodate the excess of oxygen in the network, and the disassociation of lead ions from $[FeO_4]^{-1}$ structural units during this process.

(vi) For samples containing $x \geq 50$ mol % Fe_2O_3, the apparition of new bands located in the 260–325 nm region is correlated to the possible distortion of the iron species symmetry, the presence of the larger number of Pb^{+2} ions and the apparition of the new iron species derived from the Fe_2O_3 crystalline phase, in agreement with the XRD data.

The lead ions have a pronounced affinity toward [GeO_5] and [FeO_4] structural units containing non-bridging oxygens. Our results show that the presence of fivefold germanium is a necessary transitional phase from four to sixfold germanium. At higher content of iron (III) oxide, the anomalous behavior of the germanium bonding is due to the formations of [FeO_6] structural units. When [FeO_6] structural units can no longer accommodate excess of oxygen, the Fe_2O_3 crystalline phase forms.

Density measurements

Figure 4 shows the compositional evolution of the density of iron–lead–germanate glasses. Note that the relation between the density and the iron ions content is not linear and shows important features.

(i) The density of a lead–germanate glass increases abruptly with the addition of 1 mol% Fe_2O_3. However, further increasing the Fe_2O_3 content up to 10 mol% causes the density to decrease. This can be attributed to the formation of Fe–O–Ge or Fe–O–Pb linkages with strong Fe–O ionic bonds [36], weakening the cross-linking within the glass network [37]. Further increasing the Fe_2O_3 content up to 20 mol% produces an increase in density which is linked to the conversion of [GeO_4] to [GeO_6] structural units and the formation of covalent Fe–O bonds which will lead to the open structure of the glasses.

The changes in molar volume were particularly pronounced for $x = 10\%$. We conclude that with increasing of the Fe_2O_3 content up to 10 mol%, the local environment of the germanium in the glass changes from tetrahedral to octahedral geometry.

(ii) For sample with $x > 20$ mol% Fe_2O_3, the changes in density were particularly pronounced for sample with $x = 40$ and 60 mol% and appeared to be minimal at $x = 30$ and 50 mol%. The oxygen packing density is the ratio of measured density per molecular weight and number of oxygen ions in a formula unit [38]. For $x = 40$ mol% and $x = 60$ mol%, the oxygen packing density increases which clearly indicates that the glassy network becomes tightly packed when more Fe_2O_3 is introduced to the vitreous matrix.

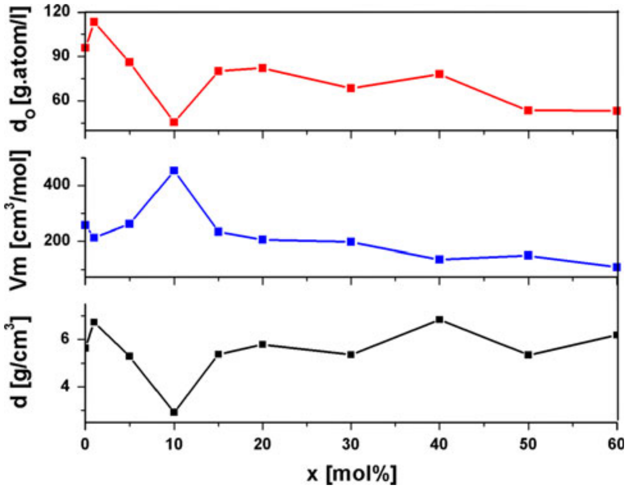

Fig. 4 Iron oxide composition dependence on **a** density, **b** molar volume, V_m, and **c** the oxygen packing density, d_O, for $x\mathrm{Fe_2O_3}\cdot(100-x)[7\mathrm{GeO_2}\cdot 3\mathrm{PbO_2}]$ samples

Conclusions

Homogeneous glasses of the $x\mathrm{Fe_2O_3}\cdot(100-x)[7\mathrm{GeO_2}\cdot 3\mathrm{PbO}]$ system were obtained from melt quenching method. We analyzed the effects of iron ions on the structure of lead–germanate glasses by FTIR and UV–VIS spectroscopy investigations. The lead network in iron–lead–germanate glasses exists in principally as $[PbO_3]$ and $[PbO_4]$ structural units while the germanate network consists from $[GeO_4]$, $[GeO_5]$, and $[GeO_6]$ structural units.

Our results show that the presence of fivefold Ge is a necessary transitional phase as the germanium environment changes from four to sixfold coordination. At higher content of iron (III) oxide, the anomalous behavior of the germanium environment is due to the conversion of some $[FeO_4]$ to $[FeO_6]$ structural units while the Pb^{+2} ions will be change compensated by association with $[GeO_5]$ structural units. The presence of the fivefold germanium is probably necessary for the formation of the $[FeO_6]$ structural units and the apparition of the Fe_2O_3 crystalline phase.

Acknowledgements The financial support of the Ministry of Education and Research of Romania-National University Research Council (CNCSIS, PN II-IDEI 183/2008, contract number 476/2009) is gratefully acknowledged by the authors.

References

1. Shepherd DP, Brick DJB, Wang J, Tropper AC, Hanna DC, Kakarantzas G, Townsend PD (1994) Opt Lett 19:954
2. Lezal D, Pedlikova J, Horak J (1996) J Non-Cryst Solids 196:178
3. Rada S, Culea M, Neumann M, Culea E (2008) Chem Phys Lett 460:196
4. Meera B, Sood A, Chandrabhas N, Ramakrishna J (1990) J Non-Cryst Solids 126:224
5. Pisarski W, Goryczka T, Wodecka-Dus B, Plonska M, Pisarska J (2005) Mater Sci Eng B 122:94
6. El-Egili K, Doweidar H, Moustafa YM, Abbas I (2003) Physica B 339:237
7. Doweidar H (1996) J Non-Cryst Solids 194:155
8. Shaw RR (1971) J Am Ceram Soc 54:170
9. Kamitsos EI, Yianopoulos YD, Karakassides MA, Chryssikos GD, Jain H (1996) J Phys Chem 100:11755
10. Murthy MK, Ip J (1964) Nature 201:285
11. Henderson GS (2007) J Non-Cryst Solids 353:1695
12. Henderson GS, Fleet ME (1991) J Non-Cryst Solids 134:259
13. Henderson GS, Wang HM (2002) Eur J Miner 14:733
14. Hussin R, Dupree R, Holland D (1999) J Non-Cryst Solids 246:159
15. Hoppe U, Kranold R, Weber HJ, Hannon AC (1999) J Non-Cryst Solids 248:1
16. Mortier M, Patriarche G (2000) J Mater Sci 35(19):4849. doi: 10.1023/A:1017512232431
17. Yang Z, Jiang Z, Liu Y, Deng Z (2006) J Mater Sci 41(18):6174. doi:10.1007/s10853-006-0159-8
18. Yang Z, Xu S, Dai S, Yang J, Hu L, Jiang Z (2004) J Mater Sci 39(11):3641. doi:10.1023/B:JMSC.0000030717.85894.69
19. Mandal S, Hazra S, Ghosh A (1994) J Mater Sci Lett 13:1054
20. Hazra S, Ghosh A (1995) J Mater Res 10(9):2374
21. Rada S, Ristoiu T, Rada M, Coroiu I, Maties V, Culea E (2010) Mater Res Bull 45:69
22. Rada S, Pascuta P, Culea M, Maties V, Rada M, Barlea M, Culea E (2009) J Mol Struct 924–926:89
23. Rada M, Maties V, Culea M, Rada S, Culea E (2010) Spectrochim Acta A 75:507
24. Rada M, Culea E, Rada S, Maties V, Pascuta P (2010) J Mater Sci 45:1487. doi:10.1007/s10853-009-4109-0
25. Shivachev BL, Petrov T, Yoneda H, Titorenkova R, Mihailova B (2009) Scr Mater 61(5):493
26. Zhang Z (1993) Phys Chem Glasses 34:95
27. Ehrt D (2004) J Non-Cryst Solids 348:22
28. Kurkjian CR, Sigety EA (1968) Phys Chem Glasses 9:73
29. Montenero A, Friggeri M, Giori DC, Belkhiria N, Pye LD (1986) J Non-Cryst Solids 84:45
30. Kurkjian CR (1970) J Non-Cryst Solids 3:157
31. Park W, Chen H (1982) Phys Chem Glasses 23:107
32. Edwards RJ, Paul A, Douglas RW (1972) Phys Chem Glasses 13:137
33. Creux S (1997) In: Proceedings on Fundamentals of Glass Science and Technology, p 41
34. Steele FN, Douglas RW (1965) Phys Chem Glasses 6:246
35. Burns RG (1993) Mineralogical applications of crystal field theory. Cambridge University, Cambridge, p 57
36. Fayon F, Bessada C, Coutures JP, Massiot D (1999) Inorg Chem 38:5212
37. Abid M, Et-labirou M, Taibi M (2003) Mater Sci Eng B 97:20
38. Srinivasa Rao N, Purnima M, Bale S, Siva Kumar K, Rahman S (2006) Bull Mater Sci 29(4):365